The Ig heavy chain protein but not its message controls early B cell development

Muhammad Assad Aslam[a,b,1], Mir Farshid Alemdehy[a,1], Bingtao Hao[c], Peter H. L. Krijger[d], Colin E. J. Pritchard[e], Iris de Rink[f], Fitriari Izzatunnisa Muhaimin[a], Ika Nurzijah[a], Martijn van Baalen[g], Ron M. Kerkhoven[f], Paul C. M. van den Berk[a], Jane A. Skok[c], and Heinz Jacobs[a,2]

[a]Division of Tumor Biology and Immunology, Netherlands Cancer Institute, 1066 CX Amsterdam, The Netherlands; [b]Institute of Molecular Biology and Biotechnology, Bahauddin Zakariya University, 60800 Multan, Pakistan; [c]Department of Pathology, New York University School of Medicine, New York, NY 10016; [d]Hubrecht Institute-Royal Netherlands Academy of Arts and Sciences (KNAW) and University Medical Center Utrecht, 3584 CT Utrecht, The Netherlands; [e]Mouse Clinic for Cancer and Aging Transgenic Facility, Netherlands Cancer Institute, 1066 CX Amsterdam, The Netherlands; [f]Genome Core Facility, Netherlands Cancer Institute, 1066 CX Amsterdam, The Netherlands; and [g]Flow Cytometry Facility, Netherlands Cancer Institute, 1066 CX Amsterdam, The Netherlands

Edited by Klaus Rajewsky, Max Delbrück Center for Molecular Medicine, Berlin, Germany, and approved October 13, 2020 (received for review March 13, 2020)

Development of progenitor B cells (ProB cells) into precursor B cells (PreB cells) is dictated by immunoglobulin heavy chain checkpoint (IgHCC), where the IgHC encoded by a productively rearranged *Igh* allele assembles into a PreB cell receptor complex (PreBCR) to generate signals to initiate this transition and suppressing antigen receptor gene recombination, ensuring that only one productive *Igh* allele is expressed, a phenomenon known as *Igh* allelic exclusion. In contrast to a productively rearranged *Igh* allele, the *Igh* messenger RNA (mRNA) (*IgHR*) from a nonproductively rearranged *Igh* allele is degraded by nonsense-mediated decay (NMD). This fact prohibited firm conclusions regarding the contribution of stable *IgHR* to the molecular and developmental changes associated with the IgHCC. This point was addressed by generating the $Igh^{Ter5H\Delta TM}$ mouse model from Igh^{Ter5H} mice having a premature termination codon at position +5 in leader exon of Igh^{Ter5H} allele. This prohibited NMD, and the lack of a transmembrane region (ΔTM) prevented the formation of any signaling-competent PreBCR complexes that may arise as a result of read-through translation across premature Ter5 stop codon. A highly sensitive sandwich Western blot revealed read-through translation of Igh^{Ter5H} message, indicating that previous conclusions regarding a role of *IgHR* in establishing allelic exclusion requires further exploration. As determined by RNA sequencing (RNA-Seq), this low amount of IgHC sufficed to initiate PreB cell markers normally associated with PreBCR signaling. In contrast, the $Igh^{Ter5H\Delta TM}$ knock-in allele, which generated stable *IgHR* but no detectable IgHC, failed to induce PreB development. Our data indicate that the IgHCC is controlled at the level of IgHC and not *IgHR* expression.

Ig heavy chain checkpoint | PreB cell antigen receptor | allelic exclusion | read-through translation | early B cell development

Early development of B lymphocytes is tightly regulated and linked to the well-defined process of variable (V), diversity (D), and joining (J) recombination, which initiates in progenitor B cells (ProB cells) (1). During this process, several DNA segments encoding V, D, and J elements of Immunoglobulin heavy chain (IgHC) are sequentially recombined, requiring Rag recombinase (2, 3). Functionally, this generates a pool of precursor B cells (PreB cells) expressing clonotypic IgH chains. A subsequent productive VJ rearrangement of an *Igk* or *Igλ* allele creates a diverse primary repertoire of membrane-bound IgM (mIgM). From an immunological perspective, this diversity enables B cells to recognize a huge variety of foreign antigens (4). Once a productive VDJ recombination event is accomplished, further rearrangement on the second *Igh* allele is inhibited, a phenomenon known as allelic exclusion (5–8). Allelic exclusion ensures that one B cell normally expresses only one specific antibody, known as the "One Cell–One Antibody" rule (9). Monoallelic expression is not only limited to *Igh* in B cells (10, 11). X chromosome inactivation (XCI) during early female embryonic development also constitutes a well-studied example of monoallelic expression, during which one of the X chromosomes is randomly silenced (12–14). This phenomenon equalizes the dosage of X-linked genes between male and female containing one and two X chromosomes, respectively (15, 16).

Several models have been proposed to explain allelic exclusion of *Igh* in B cells. According to the probabilistic asynchronous recombination model, a nonproductive *Igh* allele is relocated to pericentromeric heterochromatin region, thereby making it inaccessible for the Rag recombinase (4, 17–23). The stochastic model proposes that *Igh* rearrangement is highly efficient, but the probability of rearranging an allele in the correct reading frame encoding a pairing-competent IgHC is lower as compared to a nonproductive (out of frame) or nonpairing IgHC. According to the feedback inhibition model, the cell can sense successful *Igh* rearrangements resulting in the formation of IgHC that is subsequently assembled with surrogate light chain and the signaling components Ig-α/Ig-β into the PreB cell receptor complex (PreBCR) that initiates signals suppressing VDJ recombination (8, 24). The feedback inhibition model of allelic exclusion is based

Significance

Immunoglobulin heavy chain checkpoint (IgHCC) is a critical step during early B cell development. The role of immunoglobulin heavy chain (IgHC) at this step is well established. However, with the expanding knowledge of RNA in regulating central biological processes, there could be a noncoding contribution of IgHC mRNA (*IgHR*) in controlling the IgHCC. Here, we generated a novel mouse model that enabled us to determine a potential role of *IgHR* in the IgHCC, independent of IgHC signaling. Our data indicate that *IgHR* has no role in IgHCC and the latter is predominantly controlled by IgHC, as proposed earlier. Furthermore, this study highlights the sensitivity of progenitor B cells to low amounts of IgHC.

Author contributions: M.A.A., M.F.A., B.H., P.H.L.K., J.A.S., and H.J. designed research; M.A.A., M.F.A., B.H., P.H.L.K., F.I.M., I.N., and P.C.M.v.d.B. performed research; C.E.J.P., M.v.B., and R.M.K. contributed new reagents/analytic tools; M.A.A., M.F.A., B.H., P.H.L.K., I.d.R., P.C.M.v.d.B., J.A.S., and H.J. analyzed data; M.A.A., M.F.A. and H.J. wrote the paper; and H.J. wrote the project grant and was principal investigator.

The authors declare no competing interest.

This article is a PNAS Direct Submission.

[1]M.A.A. and M.F.A. contributed equally to this work.

[2]To whom correspondence may be addressed. Email: h.jacobs@nki.nl.

This article contains supporting information online at https://www.pnas.org/lookup/suppl/doi:10.1073/pnas.2004810117/-/DCSupplemental.

First published November 23, 2020.

on the presence of signaling-competent PreBCR and is well supported by the several mouse models that either lack the transmembrane (TM) region essential for PreBCR assembly and signaling, lack components of PreBCR itself such as lambda 5, or are deficient in PreBCR-associated downstream signaling molecules Syk and ZAP-70 (24–26). Furthermore, mice carrying mutations in Igα and Igβ, which either block their association with μIgHC or interfere with intracellular signaling cascades, also support this model (27–30). Accordingly, formation of a PreBCR is a critical IgH checkpoint (IgHCC) that is followed by clonal expansion, survival, and differentiation into PreB cells (31).

Regarding transcriptional rate, both productively and nonproductively rearranged *IgH* loci are transcribed at a similar rate (27). However, only the transcripts from a productively rearranged allele are stable and accumulate, whereas the messenger RNA (mRNA) from a nonproductively rearranged allele carrying multiple translation stop codons is subjected to nonsense-mediated mRNA decay (NMD) and thus rapidly degraded (32–34). This led us to propose an additional feedback inhibition model in which accumulation of stable coding *IgHR* is sensed by the ProB cell as a product of a productively rearranged *Igh* allele to inhibit further *Igh* rearrangements (35). In this regard, IgHC allelic exclusion could relate to XCI, which starts with the expression of a long noncoding RNA, *Xist*, from one of the two X chromosomes that will be silenced (16). Initiation of XCI is genetically controlled by the X inactivation center (*Xic*) that harbors *Xist*, which acts as a master regulator of XCI (36–39). In somatic cells, the three-dimensional (3D) distribution of *Xist* RNA domain coincides with part of the 3D space occupied by inactive X chromosome (Xi) territory (39). *Xist* accumulates *in cis* along the entire X chromosome and triggers a series of events, including chromosome-wide gene silencing, global chromatin modifications, and chromosome reorganization (40, 41). Accumulation of *Xist* on an X chromosome leads to the formation of a silent nuclear compartment that lacks RNA polymerase II and associated transcription factors (42). Gene silencing of X-linked genes by *Xist* is also determined by its ability to recruit multiple factors to Xi. Recruitment of these factors leads to the formation of facultative heterochromatin conformation (40). In mammals, nuclear periphery correlates with gene silencing. Lamin B receptor (LBR) interacts with *Xist* RNA and influences localization of Xi to nuclear lamina to facilitate its inactivation (43–45). In addition, *Xist* has been associated with its ability to influence Xi localization toward the edge of the nucleolus (46). During XCI, Xi undergoes 3D architectural changes. Circularized chromosome conformation capture (4C) analysis of transcriptionally active genes on the active X chromosome and the same silent genes on Xi show a lack of specific chromosomal interaction on Xi (47, 48). Interestingly, 3D reorganization of Xi is also dictated by *Xist* (49, 50).

To address experimentally whether the feedback inhibition of gene rearrangements in the control of *Igh* allelic exclusion is mediated only by the IgHC, or if *IgHR* also has a role in this process, we used a previously established mouse model that expresses an untranslatable form of *IgHR* by placing a premature translation termination codon at codon position +5, hence called Igh^{Ter5H} (51). This approach kept untranslated *IgHR* relatively stable, as an early premature stop codon is very inefficient in triggering NMD (51, 52). This strategy was employed to dissect the potential impact of *IgHR* from IgHC on allelic exclusion.

In our initial study (35), failure to identify any detectable IgHC from the Igh^{Ter5H} allele supported the suitability of the Igh^{Ter5H} model to study the contribution of *IgHR* in establishing allelic exclusion at *Igh*, independent of IgHC. In this system, we found that the transition of ProB cells ($CD19^+$, c-Kit^-) to PreB cells ($CD19^+$, $CD25^+$) was impaired. ProB cells were increased and PreB cells were decreased, both in relative and absolute numbers. At the same time, the frequency of ProB cells with intracellular IgHC decreased in the presence of a targeted Igh^{Ter5H} allele. Furthermore, in order to explore the effect of accumulation of *IgHR* on VDJ recombination in Igh^{Ter5H} model, recombination efficiency as measured for V to DJ rearrangement of the wild-type (WT) allele in ProB cells was quantified by two independent TaqMan PCR assays. The first assay quantified the relative frequency of the V to DJ rearrangements of the endogenous Igh^{WT} allele (product level) and the second the relative frequency of the remaining germ line D_{Q52} element (substrate level). Both assays indicated impaired recombination efficiency of Igh^{WT} allele in the $Igh^{WT/\ Ter5H}$ system. These results closely correlated with the reduced frequency of ProB cells in the $Igh^{WT/\ Ter5H}$ mouse model. In addition, independent experiments using an exogenous recombination substrate showed that impaired recombination observed in ProB cells from the Igh^{Ter5H} model was not due to reduced recombination activity. Since the initial Western blots were relatively insensitive in detecting minute amounts of IgHC encoded from the Igh^{Ter5H} allele, the results summarized above misled us in implying a contribution of *IgHR* in establishing allelic exclusion, suggesting a model in which *IgHR* might exert a noncoding function in establishing allelic exclusion, in analogy to the role of *Xist* in XCI.

The fact that *Igh* allelic exclusion is associated with ProB to PreB cell transition led us to hypothesize that the accumulation of a stable *IgHR* may contribute to initiate PreB cell differentiation. Indeed, transcriptome and *Igh* loci conformation analyses revealed that ProB cells expressing Igh^{Ter5H} mRNA acquired PreB cell features. However, detailed analyses of RNA-sequencing (RNA-Seq) data suggested the existence of a signaling-competent PreBCR in the Igh^{Ter5H} model system that was confirmed by a highly sensitive Western blot. Consequently, an optimized mouse model expressing stable Igh^{Ter5H} mRNA, lacking the TM region $Igh^{Ter5H\Delta TM}$ mouse model was generated. This would render IgHC unable to signal and thus ultimately degraded. Transcriptomic and *Igh* locus conformation analyses of $Igh^{Ter5H\Delta TM/\ Ter5H\Delta TM}$ showed that despite high expression of $Igh^{Ter5H\Delta TM}$ mRNA, the ProB cells failed to acquire PreB cell features in this setting.

In conclusion, here we provide a mouse model, $Igh^{Ter5H\Delta TM}$ that finally enabled us to determine the contribution of the *IgHR* in the IgHCC, independent of IgHC signaling potential. Our analysis showed that, apparently, *IgHR* has no obvious role in allelic exclusion and PreB cell development, which are, as proposed previously, primarily if not exclusively controlled by IgHC (8, 24). Furthermore, our results led us to conclude that locus conformation of *Igh* alleles is not influenced by *Igh* transcription but is mainly governed by PreB cell development.

Results

The Igh^{Ter5H} Knock-in Allele Triggers PreB Cell Development. Allelic exclusion is intimately linked to PreB cell differentiation, which in turn is controlled by the IgHCC, raising the question of whether early B cell differentiation can be triggered by the expression of stable *Igh* message alone. To determine if a stable Igh^{Ter5H} mRNA (35) can kick-start some aspects of early B cell development, we followed an unbiased RNA-Seq approach taking advantage of the Igh^{Ter5H} knock-in mice. We first established a PreB cell gene signature by defining all differentially expressed genes (false discovery rate [FDR] < 0.01) from WT ($CD19^+$, $B220^+$, IgM^-, c-Kit^-, $CD25^+$) PreB cells compared with $Rag1^{ko/ko}$ ProB cells (Fig. 1*A*). Having established this PreB cell signature, we compared the mRNA expression profiles of differentiation-arrested ProB cells from $Igh^{Ter5H/Ter5H}$ with those of $Rag1^{ko/ko}$ mice. This comparison indicated clear features of advanced differentiation in the Igh^{Ter5H} setting (Fig. 1*B*). Strikingly, among differentially upregulated genes, we identified *Ikzf3*, *Il2ra* (*CD25*), *CD2*, and *CD22* (Fig. 1*C*). Importantly, these genes are normally associated with a signaling-competent PreB cell receptor (53). In order to exclude any contribution of RAG, we compared $Igh^{Ter5H/wt}$;$Rag1^{ko/ko}$ with $Rag1^{ko/ko}$. This comparison showed that the developmentally

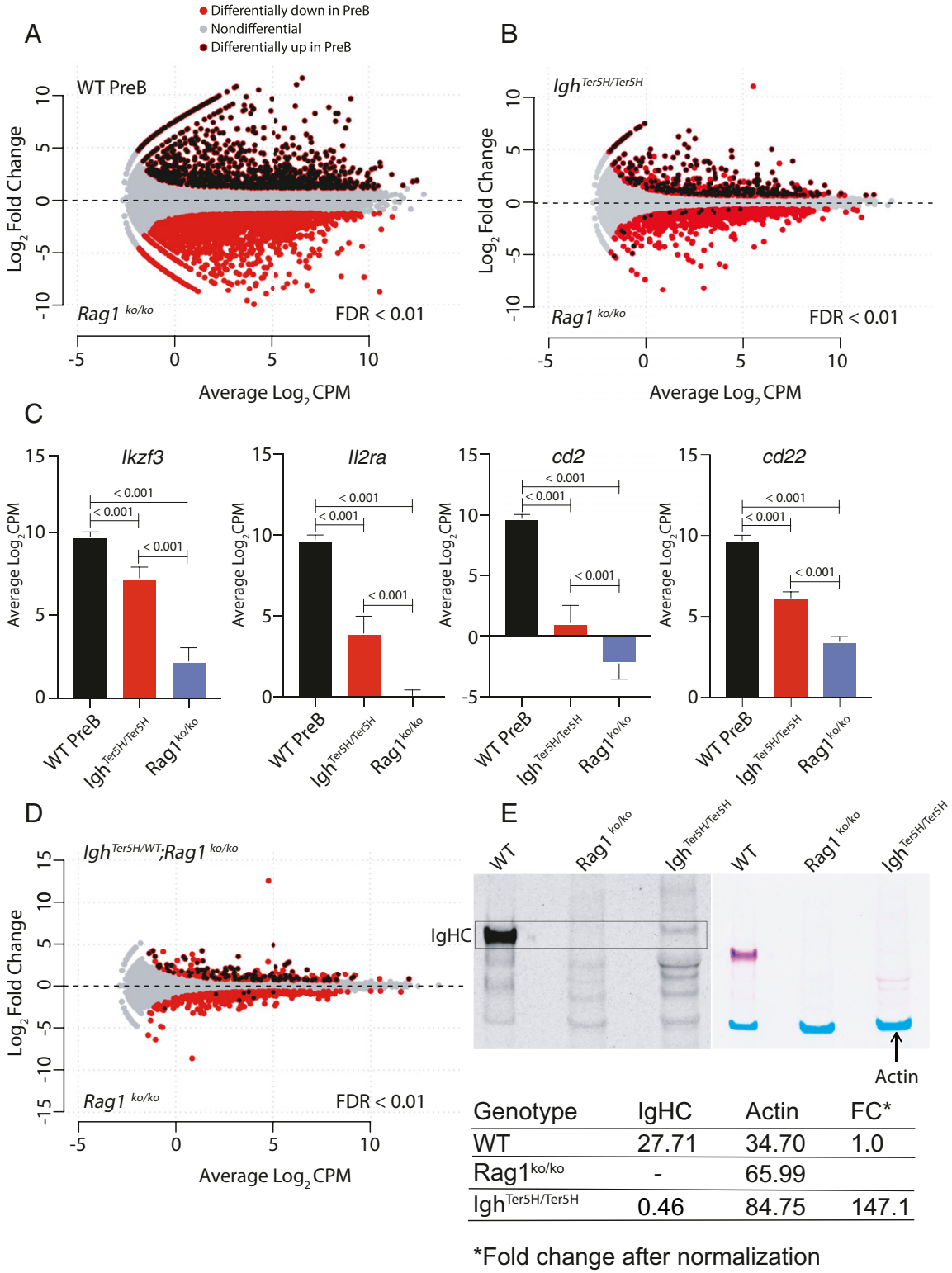

Genotype	IgHC	Actin	FC*
WT	27.71	34.70	1.0
Rag1$^{ko/ko}$	-	65.99	
Igh$^{Ter5H/Ter5H}$	0.46	84.75	147.1

*Fold change after normalization

Fig. 1. Induction of PreB cell markers in the *Igh*^{Ter5H} knock-in system is triggered by minute traces of IgH chain protein. (*A*) MA plot generated from RNA-Seq data showing differential gene expression (FDR < 0.01) between WT PreB and *Rag1*$^{ko/ko}$ ProB cells to establish PreB cell gene signature. (*B*) MA plot showing relative enrichment of PreB cell gene signature in *Igh*$^{Ter5H/Ter5H}$ compared with *Rag1*$^{ko/ko}$. (*C*) The average $\log_2$ counts per million after trimmed mean of M-values normalization and removing the batch effect using voom function under the limma and edgeR package shows the mRNA expression of *Ikzf3*, *Il2ra*, *cd2*, *and cd22*. The genetic background of ProB cells (c-Kit$^+$, CD25$^-$) of the indicated genotypes and wild-type PreB cells (c-Kit$^-$, CD25$^+$) are indicated. The FDR shows the statistical significance. Differences with an FDR < 0.05 are considered significant. (*D*) MA plot showing relative enrichment of PreB cell gene signature in *Igh*$^{Ter5H/Ter5H}$ and *Igh*$^{Ter5H/WT}$;*Rag1*$^{ko/ko}$ compared with *Rag1*$^{ko/ko}$. (*E*) Western blot showing the presence of trace amounts of IgHC in *Igh*$^{Ter5H/Ter5H}$ system is indicated on the right. Actin is shown as a loading control on the left. The reduction in IgHC *in Igh*$^{Ter5H/Ter5H}$ is shown as fold change after normalization to WT.

advanced features shown in Igh^{Ter5H} arise independently of RAG (Fig. 1*D*).

PreB Cell Development in Igh^{Ter5H} Knock-in System Does Not Exclude IgHC Contribution. A substantial fraction of PreB cell markers was found induced in the Igh^{Ter5H} knock-in system, which led us to consider two possibilities: Either stable IgHR expression initiates differentiation, or, given the existence of read-through translation, previously undetected minute amounts of IgHC might be generated that suffice to induce developmental progression (35). To distinguish between these possibilities, we established a highly sensitive sandwich Western blot system. Using a polyclonal donkey anti-goat to detect a polyclonal goat anti-mouse IgM antibody, we found detectable amounts of IgHC in B cell progenitors from the $Igh^{Ter5H/Ter5H}$ model, which were 147-fold reduced compared with WT (Fig. 1*E*). Apparently, while a premature stop codon at position +5 allows stable mRNA expression, it appeared insufficient in preventing translation. The failure to dissect the contribution of IgHR and IgHC in PreB cell development required further optimization of the $Igh^{Ter5H/Ter5H}$ system.

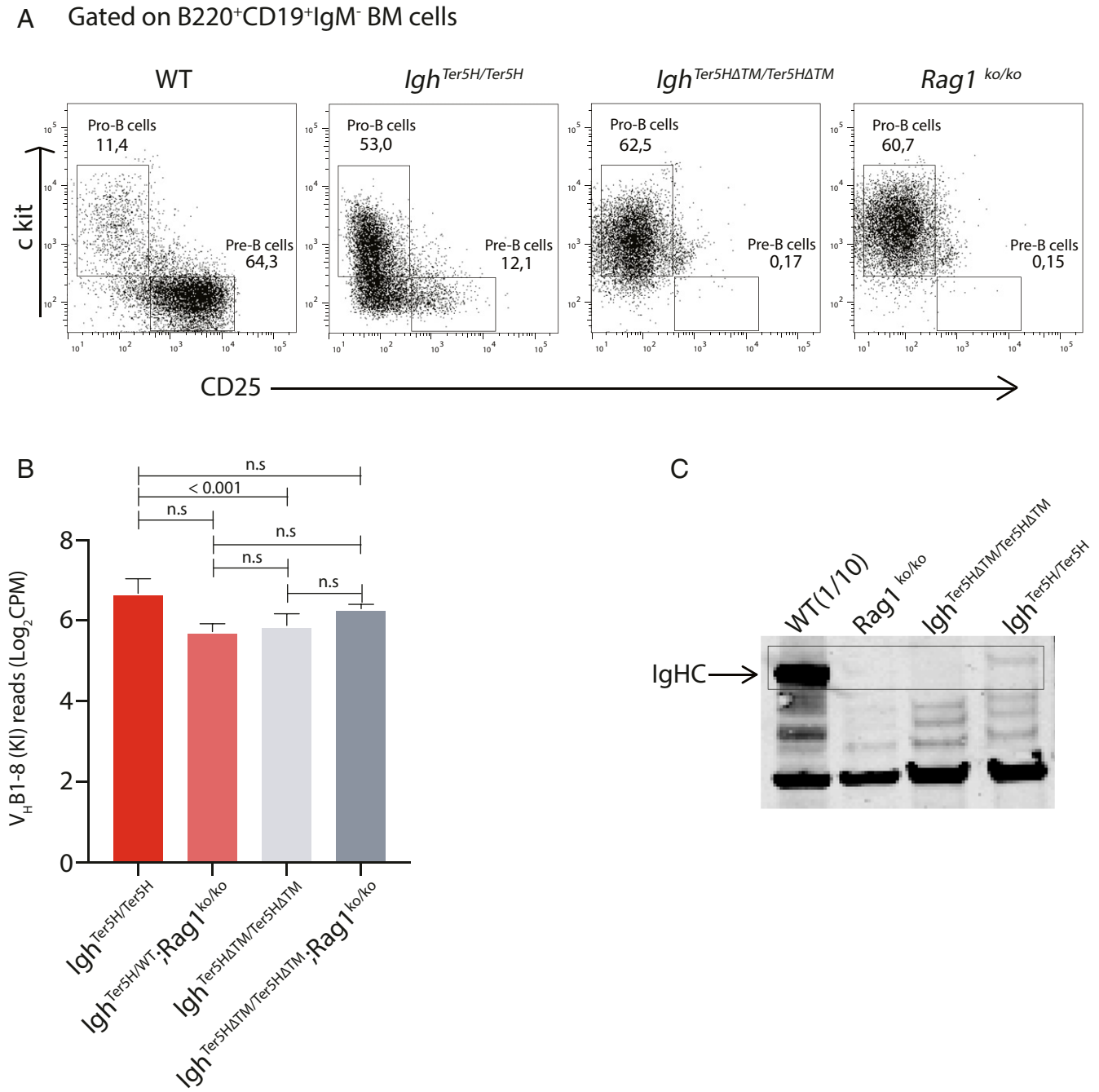

Fig. 2. $Igh^{Ter5H\Delta TM/Ter5H\Delta TM}$ system shows stable $Igh^{Ter5H\Delta TM}$ mRNA expression but no detectable trace of IgH chain protein. (*A*) FACS identification of ProB (c-Kit$^+$, CD25$^-$) and PreB cells (c-Kit$^-$, CD25$^+$) from bone marrow of the respective mice genotypes. (*B*) The average $\log_2$ counts per million after trimmed mean of M-values normalization and removing the batch effect using voom function under the limma and edgeR package shows the mRNA expression of the targeted *VHB1.8* knock-in allele. The FDR indicates the statistical significance. The difference with FDR less than 0.05 is considered significant. (*C*) Western blot confirming the degradation of IgHC in the $Igh^{Ter5H\Delta TM/Ter5H\Delta TM}$ system. n.s., nonsignificant.

Generation of $Igh^{Ter5H\Delta TM/Ter5H\Delta TM}$ Knock-in Mice from the $Igh^{Ter5H/Ter5H}$ Model and Its Validation. Knowing that the TM region of membrane-bound IgHC is essential for PreBCR assembly and signaling (54), we deleted the TM exon in the Igh^{Ter5H} locus (*SI Appendix*, Fig. S1 *A* and *B*). To accomplish this goal, we first derived mouse embryonic stem cells from blastocysts isolated from super ovulated $Igh^{Ter5H/Ter5H}$ mice. Subsequently, an $Igh^{Ter5H\Delta TM}$ knock-in allele was derived from the $Igh^{Ter5H/Ter5H}$ embryonic stem

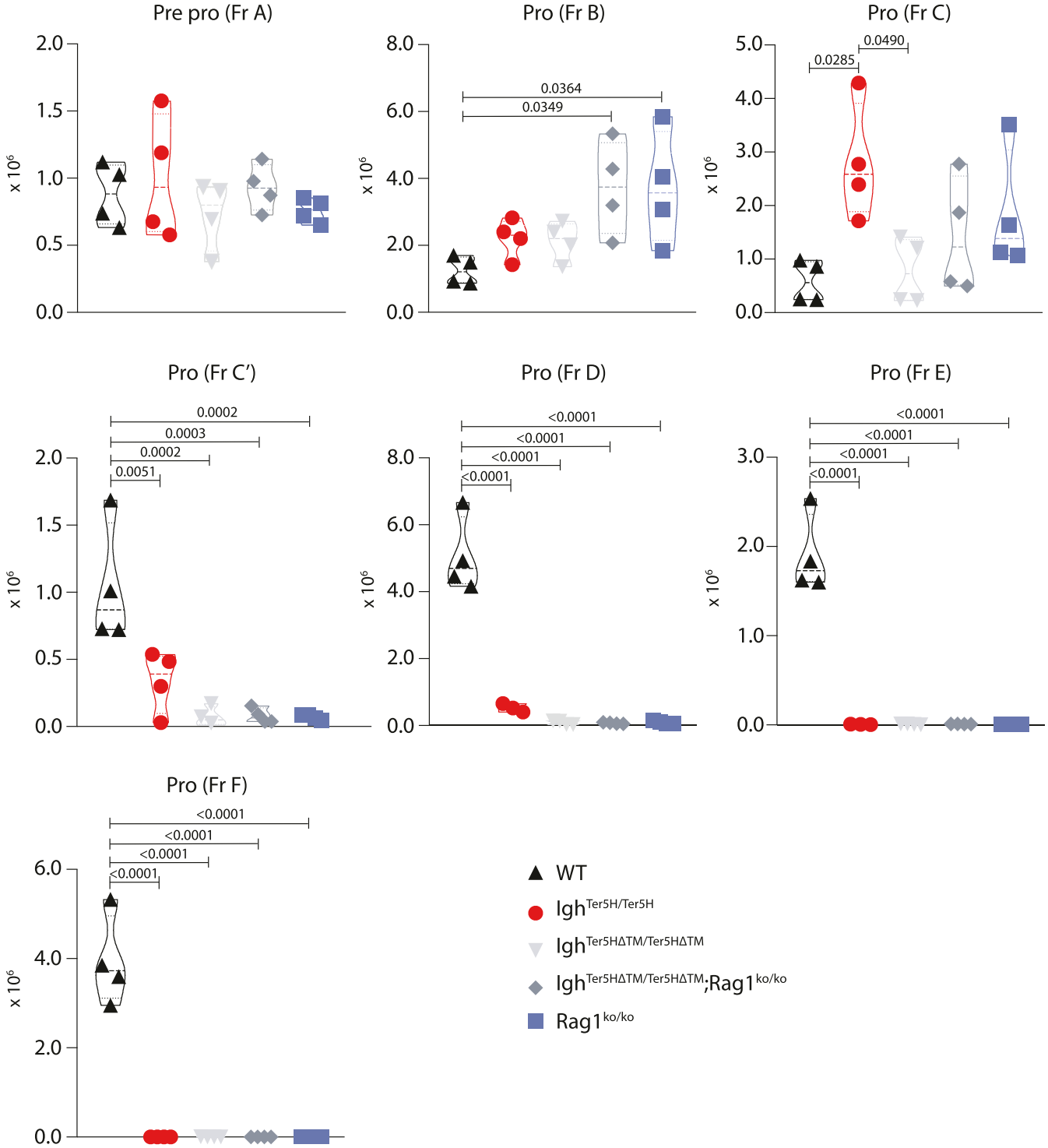

Fig. 3. ProB cells from $Igh^{Ter5H/Ter5H}$, $Igh^{Ter5H\Delta TM/Ter5H\Delta TM}$, and $Igh^{Ter5H\Delta TM/Ter5H\Delta TM}$;$Rag1^{ko/ko}$ predominately arrest at Fraction C. The violin plot represents the absolute numbers of total nucleated cells of B cell subsets from bone marrow (Fractions A, B, C, C′, D, E, and F, according to Philadelphia staining) for each genotype. Each data point represents the value from an individual mouse. ROUT (robust regression and outlier removal) method in GraphPad Prism under default settings is used to identify outliers from the data, which are removed for the subsequent analysis. A one-way ANOVA test with Tukey's multiple comparison test was applied to calculate the *P* value to determine the statistical significance. $P < 0.05$ is considered statistically significant, and only the significant values are shown. Fr, Fraction.

cells using Crispr-Cas9 and specific guide RNAs (gRNAs) targeting the flanking region of the TM exon. $Igh^{Ter5H\Delta TM}$ knock-in clones were injected into C57B/J6 blastocysts to generate chimeric mice and introduce the mutation into the germ line (*SI Appendix*, Fig. S1*C*).

This strategy ensured that the open reading frame (ORF) and thus the stability of the *IgHR* remain intact, but any residual read-through translation product is incapable of PreBCR assembly and signaling. RNA-Seq data confirmed an abundant expression of $Igh^{Ter5H\Delta TM}$ mRNA in the ($CD19^+$, $B220^+$, IgM^-, c-Kit^+, $CD25^-$) ProB cells from $Igh^{Ter5H\Delta TM/Ter5H\Delta TM}$ mice (Fig. 2*B*). To confirm the absence of IgHC in ProB cells in a homozygous $Igh^{Ter5H\Delta TM}$ setting (54), we repeated the sandwich Western blot on lysates prepared from ProB cells from $Igh^{Ter5H\Delta TM/\ Ter5H\Delta TM}$ knock-in mice. The absence of detectable levels of IgHC validated our system (Fig. 2*C*). Having excluded IgHC expression and at the same time confirmed the stability of the $Igh^{Ter5H\Delta TM/\ Ter5H\Delta TM}$ mRNA, we now had a system in hand to study the role of $Igh^{Ter5H\Delta TM}$ mRNA in controlling PreB cell development in the absence of IgHC.

PreB Cell Development Is Predominantly Controlled by the IgHC and Not *IgHR*. To determine in more detail the developmental stage in which B cell precursors become arrested, we performed Philadelphia staining (55), which enables a detailed characterization of PreB cell subsets, specifically a separation into Pre–Pro B cells (Fraction A), ProB cells (Fraction B and C), and the PreB cell fractions comprising large, early PreB cells (Fraction C′) and small late PreB cells (Fraction D). These analyses revealed that at the cellular level, B cell precursors from $Igh^{Ter5H/Ter5H}$, $Igh^{Ter5H\Delta TM/\ Ter5H\Delta TM}$, and $Igh^{Ter5H\Delta TM/Ter5H\Delta TM}$;$Rag1^{ko/ko}$ mice behaved like those from $Rag1^{ko/ko}$ mice, where B cell progenitors arrest at Fraction C (Fig. 3 and *SI Appendix*, Fig. S2 *A* and *B*).

To provide an in-depth analysis of the potential contribution of *IgHR* in controlling early onset of PreB cell development, we compared the transcriptomes between ProB cells from $Igh^{Ter5H\Delta TM/\ Ter5H\Delta TM}$ and $Rag1^{ko/ko}$ mice. We observed that most PreB cell markers identified in the $Igh^{Ter5H/Ter5H}$ setting were no longer differentially expressed in $Igh^{Ter5H\Delta TM/Ter5H\Delta TM}$ mice (Fig. 4*A*). To further exclude any confounding issue related to RAG expression, the $Igh^{Ter5H\Delta TM}$ knock-in allele was introduced into the $Rag1^{ko/ko}$ background to generate $Igh^{Ter5H\Delta TM/Ter5H\Delta TM}$;$Rag1^{ko/ko}$ mice (Fig. 4*B*). In order to determine the contribution of PreB cell signature genes found in differentially up-regulated genes in arrested ProB cells from $Igh^{Ter5H/Ter5H}$, $Igh^{Ter5H\Delta TM/Ter5H\Delta TM}$, $Igh^{Ter5H/WT}$;$Rag1^{ko/ko}$, and $Igh^{Ter5H\Delta TM/Ter5H\Delta TM}$;$Rag1^{ko/ko}$ mice, we compared those to ProB cells from $Rag1^{ko/ko}$ mice. To provide the relative overlap of ProB cells from different genotypes with the WT PreB cell, we normalized those according to the actual number of genes in the PreB cell signature (Fig. 4*C*). This analysis clearly indicated that among all of the genotypes, ProB cells from $Igh^{Ter5H\Delta TM/Ter5H\Delta TM}$;$Rag1^{ko/ko}$ have the least overlap with PreB cells. Only 9 of the 1,247 genes (0.7%) that defined the PreB cell signature were differentially expressed in $Igh^{Ter5H\Delta TM/Ter5H\Delta TM}$;$Rag1^{ko/ko}$. The same analysis revealed that 10% of the genes that were differentially up-regulated in $Igh^{Ter5H/WT}$;$Rag1^{ko/ko}$ compared with $Rag1^{ko/ko}$ belong to PreB cell signature (Fig. 4*D*). Most relevant regarding a potential role for *IgHR* in the IgHCC, a nonsignificant difference in the steady-state level of *IgHR* between $Igh^{Ter5H\Delta TM/Ter5H\Delta TM}$;$Rag1^{ko/ko}$ and $Igh^{Ter5H/WT}$;$Rag1^{ko/ko}$ was found (Fig. 3*B*). These results led us to conclude that irrespective of its high expression, the $Igh^{Ter5H\Delta TM}$ message does not contribute to PreB cell differentiation. In order to determine the magnitude of similarity among different genotypes, Pearson correlation coefficient was calculated based on the expression of protein coding genes (*SI Appendix*, Table S1). Hierarchical clustering revealed that both $Igh^{Ter5H/Ter5H}$ and $Igh^{Ter5H/WT}$;$Rag1^{ko/ko}$ clustered closer to WT PreB cells irrespective of batches. On the contrary, $Igh^{Ter5H\Delta TM/\ Ter5H\Delta TM}$ and $Igh^{Ter5H\Delta TM/\ Ter5H\Delta TM}$;$Rag1^{ko/ko}$ clustered together with $Rag1^{ko/ko}$, again irrespective of different batches (Fig. 4*E*). This analysis further strengthened our conclusion about the role of *Igh* message in PreB cell differentiation.

***Igh* Locus: Chromatin Conformation Is Predominantly Ruled by Differentiation and Not Transcription.** The $Igh^{Ter5H\Delta TM}$ mRNA expression failed to induce transcriptional changes associated with PreB cell differentiation. However, apart from transcriptional changes, PreB cell differentiation is associated with defined topological changes at the *IgH* locus. During the transition from ProB to PreB cell differentiation, the *IgH* locus changes from a contracted to a decontracted configuration in ProB and PreB cells, respectively (17, 18, 21). In order to determine if differentiation or transcription is responsible for the local conformational changes in *Igh* locus, the distance between two probes located at the two ends of *Igh* locus was measured using fluorescence in situ hybridization. Of note, except for the deleted 332-base-pair fragment containing the TM exon, the transcriptional units of both Igh^{Ter5H} and $Igh^{Ter5H\Delta TM}$ loci were kept identical. This excluded any confounding issues related to regulatory elements of the modified *Igh* locus that may influence the results. Our analyses revealed that despite high $Igh^{Ter5H\Delta TM}$ mRNA expression, the *Igh* locus remained relatively contracted compared with the Igh^{Ter5H} (Fig. 5 *A* and *B*). This suggests that *Igh* locus decontraction is associated with the PreB cell stage and not dictated by *Igh* transcription or the *Igh* transcript.

Discussion

The IgHCC represents a critical, tightly regulated step in early B cell development. The developmental transition from a ProB to a PreB cell strictly depends on the somatic generation of a productive rearrangement of a V gene segment to one of the two preexisting DJ-rearranged *Igh* alleles in ProB cells (56). The ProB cell becomes developmentally arrested if rearrangement is unsuccessful, leading to apoptosis (27). Successful rearrangement leads to PreB cell differentiation in which further rearrangements at the *Igh* alleles are prohibited, ensuring "allelic exclusion." This phenomenon provides the exquisite antigen specificity of B cell–mediated immune responses. According to the feedback model, the IgHC protein encoded by productively rearranged VDJ join, that is, the IgHC is sensed by the cell and prohibits further rearrangements at both *Igh* alleles (8, 24).

Our previous studies with Igh^{Ter3} transgenic and Igh^{Ter5} knock-in mouse models implicated a contribution of the *Igh* message in establishing allelic exclusion. This led us to propose an alternate feedback inhibition model in which the accumulation of a stable mRNA from a productive VDJ rearrangement is sensed by the cells to prevent further rearrangement (35). In contrast, transcripts from a nonproductively rearranged allele are subject to NMD and cannot initiate this feedback inhibition.

Based on the tight coordination between early B cell development and allelic exclusion, we aimed to explore the developmental changes that might be governed by stable *IgHR* in the absence of IgHC. However, detailed transcriptional analyses and highly sensitive Western blot analyses revealed minute amounts of IgHC. Apparently, an *IgHR* with a premature translational stop codon can be processed via read-through translation. This observation indicated that previous conclusions required further exploration, necessitating the generation of a new mouse model that could dissect the role of *IgHR* from IgHC during early B cell development.

Extensive transcriptional analyses of the new model revealed that the IgHCC is not controlled by *IgHR*. Furthermore, our data strongly suggest that conformational changes at the *Igh* locus are regulated by developmental rather than transcriptional circuits. Our results indicate that ProB cells are apparently highly effective in sensing minute amounts of IgHC that arise as a result of

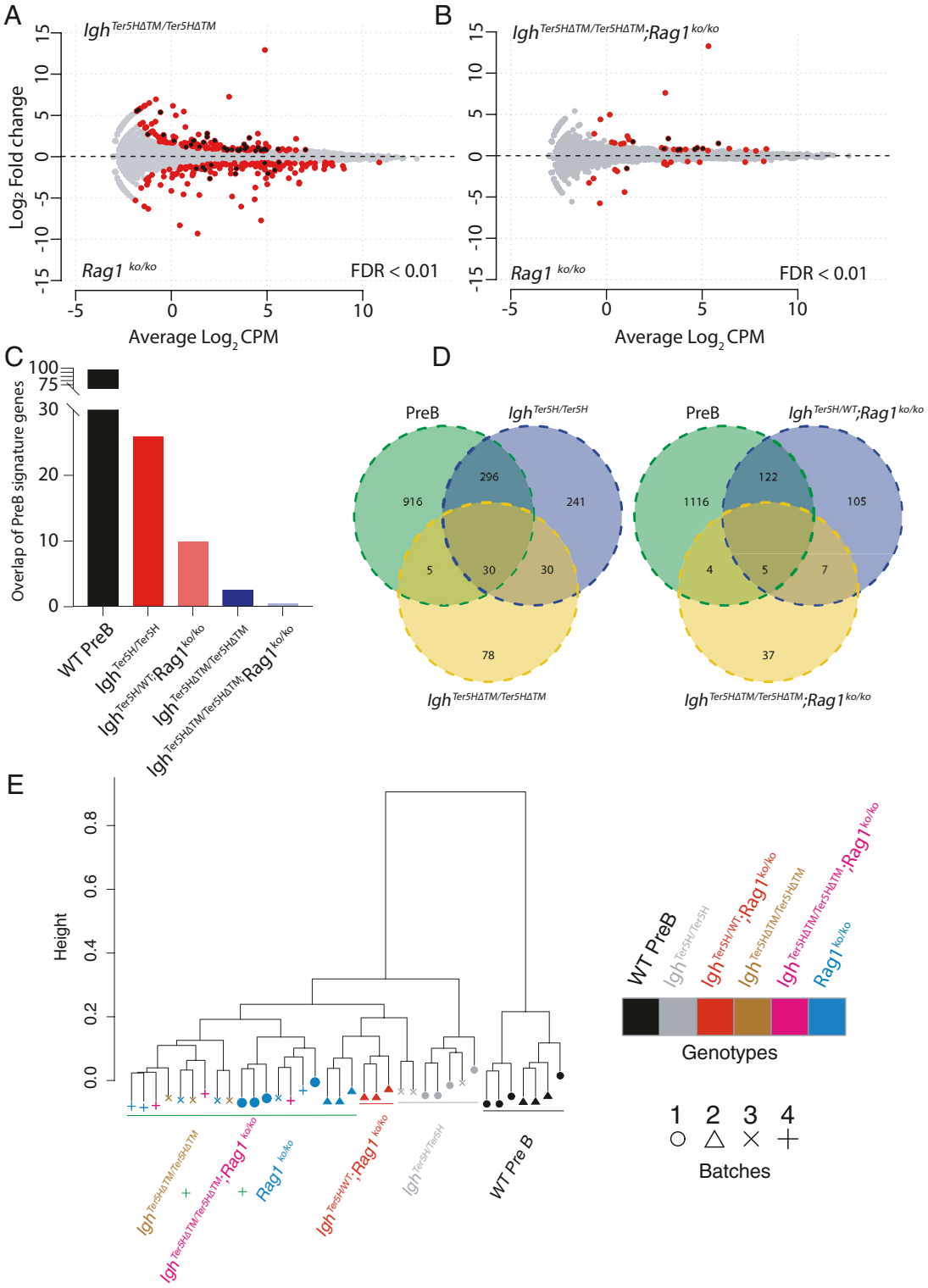

Fig. 4. The $Igh^{Ter5H\Delta TM/Ter5H\ \Delta TM}$ knock-in fails to induce PreB cell markers. (*A* and *B*) MA plots displaying a minor fraction of PreB cell signatures differentially expressed in $Igh^{Ter5H\Delta TM/Ter5H\Delta TM}$ and $Igh^{Ter5H\Delta TM/Ter5H\Delta TM};Rag1^{ko/ko}$ system compared with $Rag1^{ko/ko}$. (*C*) Relative percentage of PreB cell signature genes differentially expressed in ProB cells from different models when compared with $Rag1^{ko/ko}$ ProB cells. (*D*) Venn diagrams showing the number of common genes among the mentioned genotypes. (*E*) Hierarchical clustering analysis based on Pearson correlation coefficient values calculated from the expression values of protein coding genes showing the magnitude of similarity among different genotypes.

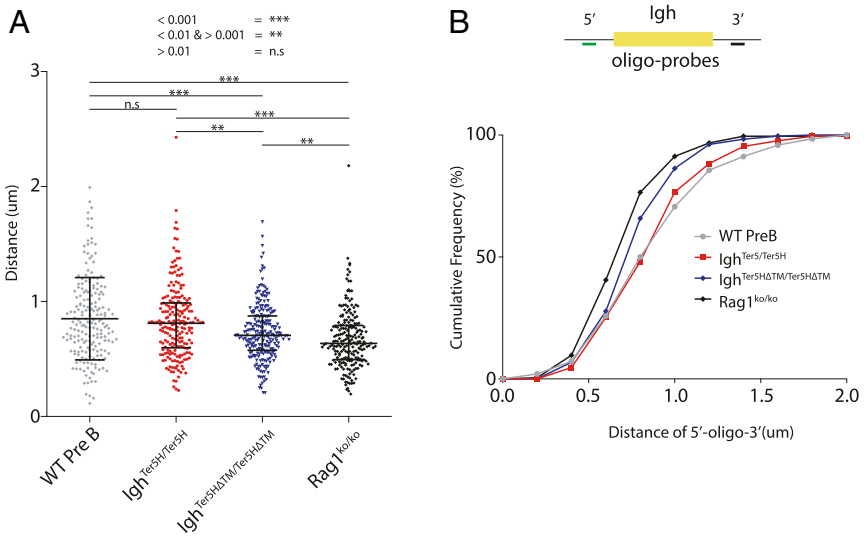

Fig. 5. *Igh*$^{Ter5H\Delta TM/Ter5H\Delta TM}$ system shows contracted conformation of *Igh* loci. (*A*) Scatter dot plot shows the distribution of distances determined between two oligo probes on distal ends of *Igh* locus as measured by fluorescence in situ hybridization for ProB cells (c-Kit$^+$, CD25$^-$) of the indicated genotypes and wild-type PreB cells (c-Kit$^-$, CD25$^+$). Data are presented as mean ± SD. Statistical significance is determined by the *P* value calculated by unpaired Student's *t* test with two-tailed distributions. $P < 0.01$ is considered statistically significant. (*B*) The graph displays the cumulative frequency percentage of all of the data points for a given distance. n.s., nonsignificant.

read-through translation. Apparently, this level of translation can initiate but not complete the developmental progression toward PreB cells. In addition, the very low amounts of IgHC in the Ter5H system may also be due to the active degradation of IgHC associated with PreB cell development (57–60), which may further contribute to its low expression (35). Compared with signaling-deficient models that may still be able to provide some signal, we present an efficient system in which trace amounts of signaling-incompetent, PreBCR assembly–deficient IgHC initially produced by read-through translation becomes rapidly degraded, and thus only the effect of stable *IgHR* could be addressed.

Finally, these insights strongly support the initial feedback model in which the IgHC is required to control allelic exclusion and drive early B cell development (4, 8, 24). These data are in line with previous observations made in the T cell lineage, in which the TCR-β chain but not a frame-shifted message controls rearrangement and early T cell development (61). Using advanced technology, we here extend these findings to the B cell lineage and arrived at very similar conclusions. These data reveal that both productive as well as nonproductive *IgHR* do not trigger PreB cell differentiation. Considering the common origin of lymphocytes and the similarity regarding their developmental trajectories, except a few differences such as absence of receptor editing in T cells, at large, both systems apparently follow similar molecular paths in regulating early development.

Conclusion

The IgHC rather than its stable message controls early B cell development. Our findings that the *IgHR* apparently does not exert a noncoding function indicates that the IgHCC is established only by IgHC and thus is distinct from XCI, which is predominantly controlled by the long noncoding RNA *Xist*. We propose that the ability to sense signaling-competent preBCR and translate this into rapid B cell development is key in establishing allelic exclusion at the IgH locus as initially proposed (8, 24). This high sensitivity provides a strong argument that *Igh* allelic exclusion, *Igh* locus conformation (this study), Rag expression (62), and differentiation are tightly linked and not affected by *Igh* transcription. The current study also highlights the biological significance of read-through translation.

Methods

Generation of *Igh*$^{Ter5H\Delta TM}$ Mouse Model. To generate *Igh*$^{Ter5H\Delta TM}$ mouse model, we first derived mouse embryonic stem cells from blastocyst isolated from super ovulated *Igh*$^{Ter5H/Ter5H}$ mice. Region flanking TM1 at *Ter5H* locus was targeted by Crispr-Cas9. Embryonic stem (ES) cells were transfected with a pX330 plasmid encoding specific gRNAs (CCGTCTAGCTTGAGCTATT and ACAAGTGGACAGCAATTCAC) and Cas9. gRNAs were designed using the https://zlab.bio/guide-design-resources tool. Subsequently, clones with the desired deletion of the TM region were selected by PCR and injected into C57B/J6 blastocysts. Chimeric mice were crossed to C57B/J6, and the offspring were tested for germ line transmission of the *Igh*$^{Ter5H\Delta TM}$ knock-in allele. *Igh*$^{Ter5H\Delta TM}$ knock-in mice were maintained on a C57B/J6 background to exclude confounders related to the genetic background. All mice used for this were maintained under specific pathogen-free conditions at the animal laboratory facility of the Netherlands Cancer Institute (NKI; Amsterdam, Netherlands). Mice used for experiments were between 6 and 8 wk old and of both genders. All experiments were approved by the Animal Ethics Committee of the NKI and performed in accordance with the Dutch Experiments on Animals Act and the Council of Europe.

Genotyping PCR. Mice were genotyped for the deletion of the TM region using the forward primer (*Igh*$^{Ter5H\Delta TM}$-FWD: GGTAGGACAAGCAACGCACGGG) and reverse primer (*Igh*$^{Ter5H\Delta TM}$ -REV: CCTTGCGGCCGCCCATG TGACATTTGTTTACAGC). The WT allele was identified as a PCR product of 960 base pairs, while *Igh*$^{Ter5H\Delta TM}$ allele produced a 628-base-pair DNA fragment. Rag1 status was detected by using the combination of the forward primer 1 (Rag1-FWD1: GGCTTAGACACTTCTGCCGCATCTGTGG), reverse primer 1 (Rag1-REV1: CTGACCCTAGCCTGAGTTCTCTTGCGAC), reverse primer 2 (Rag1-REV2: CCAC CACTGTGAAGGGACCATTCAGGTAG), and reverse primer 3 (Rag1-REV3: CTACCGGTGGATGTG GAATGTGTGCGAG).

Flow Cytometry and Sorting. For flow cytometry experiments, two femurs and two tibiae from each mouse were used to isolate bone marrow, but for sorting, both the hip bones were also used. Single-cell suspensions were made from bone marrow, and the cells were subjected to erythrocyte lysis for 1 min on ice. Following erythrocyte lysis, the cells were stained with a mixture of fluorescently labeled antibodies for 30 min on ice in the dark to identify distinct cellular populations. The 7-AAD– or Zombie NIR–positive cells were identified as dead cells and were excluded from the analysis. Zombie NIR stock was prepared in dimethyl sulfoxide according to the manufacturer's instructions. For staining with Zombie NIR, the cells were washed with phosphate-buffered saline (PBS) and then stained for 20 min on ice in the dark with Zombie NIR diluted in PBS. All monoclonal antibodies used for flow cytometry experiments and sorting are shown along with their respective clone, conjugated

fluorochrome, dilution, and vendor (*SI Appendix*, Table S2). For cell sorting and the analysis for Fig. 2*A* and *SI Appendix*, Fig. S3, the antibodies mix was prepared in PBS carrying 0.5% bovine serum albumin, 2mM ethylenediaminetetraacetic acid, and 0.02% Azide. For the analysis for *SI Appendix*, Fig. S2, the antibody mix was prepared in a brilliant stain buffer (catalog number 566349) that was purchased from BD Bioscience. The 7-AAD was added to prestained cells just before fluorescence-activated cell sorting (FACS) measurement. The specific cell population was sorted by FACSAria IIu (BD Bioscience), FACSAria Fusion (BD Bioscience), or MoFlo Astrios (Beckman Coulter) in fetal calf serum (FCS) precoated tubes. Flow cytometry was performed using the LSR Fortessa (BD Biosciences), and data were analyzed with FlowJo software (Tree Star Inc. and BD Biosciences).

Fluorescence In Situ Hybridization. Bacterial artificial chromosome (BAC) probes CT7-34H6 (3′ *Igh*) and RP24-386J17 (5′ *Igh*) were labeled by nick translation with ChromaTide Alexa Fluor 488 or 594-5-UTP (Molecular Probes). The oligo probes covering the entire *Igh* locus were ordered from Arbor Biosciences. For one coverslip, 0.5 μg of nick-translation product and 15 pmol of oligo probes were precipitated and resuspended in 10 μl of hybridization buffer (50% formamide/20% dextran sulfate/5 × Denhardt's solution), denatured for 5 min at 95 °C, and preannealed for 45 min at 37 °C before overnight hybridization with cells. The 3D images were acquired by confocal microscopy on a Leica SP5 Acousto-Optical Beam Splitter system. Optical sections separated by 0.3 μm were collected, and stacks were analyzed using ImageJ software.

RNA-Seq Sample Preparation. Sorted cells were resuspended in TRIzol (Ambion Life Technologies), and total RNA was extracted according to the manufacturer's protocol. Quality and quantity of the total RNA was assessed by the 2100 Bioanalyzer using a nano chip (Agilent). Only RNA samples with an RNA Integrity Number > 8 were subjected to library generation.

RNA-Seq Library Preparation. Strand-specific complementary DNA (cDNA) libraries were generated using the TruSeq Stranded mRNA sample preparation kit (Illumina) according to the manufacturer's protocol. The libraries were analyzed for size and quantity of cDNAs on a 2100 Bioanalyzer using a DNA 7500 chip (Agilent), diluted, and pooled in multiplex sequencing pools. The libraries were sequenced as 65 base single reads on a HiSeq2500 (Illumina).

RNA-Seq Preprocessing. Strand-specific RNA reads (11 to 33 million reads per sample), 65-base-pair single-end, were aligned against the mouse reference genome (Ensembl build 38) using Tophat (version 2.1, bowtie version 1.1). Tophat was supplied with a Gene Transfer Format (GTF) file (Ensembl version 77) and was supplied with the following parameters: `–prefilter-multihits – no-coverage-search – bowtie1 –library-type fr-firststrand`. In order to count the number of reads per gene, a custom script which is based on the same ideas as HTSeq-count was used. A list of the total number of uniquely mapped reads for each gene that is present in the provided GTF file was generated.

Gene Expression Analysis. Differential expression analysis was performed in R language (version 3.5.1) using edgeR package. Default arguments were used with the design set to specific genotypes. Genes that have no expression across all samples within the dataset were removed. Analysis was restricted to genes that have least a 2 counts per million (cpm) value in all samples in specific contrasts to exclude very-low-abundance genes. Immunoglobulin heavy variable (*Ighv*) genes were excluded to avoid any confounding issue. The FDR was determined after the Benjamini-Hochberg multiple testing correction. Genes with an FDR below 0.01 were considered to be differentially expressed. Sets of differentially expressed genes in indicated conditions were called gene signatures. MA (ratio intensity) plots were generated after carrying differential expression analysis done by the edgeR package (63, 64). Counts were shown as the average $\log_2$ cpm after trimmed mean of M-values normalization and removing the batch effect. Batch effects were corrected by voom function under the limma (3.44.3) and edgeR package. For calculating Pearson correlation, only protein coding genes with a cpm value greater than 2 in all of the samples were taken. After correcting for the batch effect and library normalization, Pearson correlation was calculated using cor function in R with the default parameters. The correlation values were used to conduct hierarchical clustering analysis. Hierarchical clustering analysis was done by the hclust function in R, and the dendrogram was visualized by using the dendosort package (0.3.3). The RNA-Seq datasets reported in this article have been deposited at the National Center for Biotechnology Information under the accession number GSE144275 (Token number: ijwxusygpdwhbqh).

Statistics. Statistical analyses for Figs. 3 and 5*A* were performed using GraphPad Prism (version 8.0.0).

Data Availability. All study data are included in the article and supporting information.

ACKNOWLEDGMENTS. The authors would like to thank the NKI genomics core facility for library preparations and sequencing, the NKI Flow Cytometry facility for assistance, and the caretakers of the NKI Animal Laboratory facility for assistance and excellent animal care. We gratefully acknowledge Ramen Bin Ali from the Mouse Clinic for Cancer and Aging Transgenic Facility for his help in generating $Igh^{Ter5H\Delta TM}$ knock-in mice and Abi Pataskar for bioinformatic discussions. We would like to thank Jonathan Yewdell for pointing out that read-through translation is effective in immune cells. This project was made possible by a generous TOP grant from the Netherlands Organisation for Scientific Research (NWO) ZonMW (91213018) to H.J. The funders had no role in study design, data collection and interpretation, or the decision to submit the work for publication.

1. H. Igarashi, S. C. Gregory, T. Yokota, N. Sakaguchi, P. W. Kincade, Transcription from the RAG1 locus marks the earliest lymphocyte progenitors in bone marrow. *Immunity* **17**, 117–130 (2002).
2. D. B. Roth, J. P. Menetski, P. B. Nakajima, M. J. Bosma, M. Gellert, V(D)J recombination: Broken DNA molecules with covalently sealed (hairpin) coding ends in scid mouse thymocytes. *Cell* **70**, 983–991 (1992).
3. J. F. McBlane *et al*., Cleavage at a V(D)J recombination signal requires only RAG1 and RAG2 proteins and occurs in two steps. *Cell* **83**, 387–395 (1995).
4. D. Jung, C. Giallourakis, R. Mostoslavsky, F. W. Alt, Mechanism and control of V(D)J recombination at the immunoglobulin heavy chain locus. *Annu. Rev. Immunol.* **24**, 541–570 (2006).
5. C. Vettermann, M. S. Schlissel, Allelic exclusion of immunoglobulin genes: Models and mechanisms. *Immunol. Rev.* **237**, 22–42 (2010).
6. B. Pernis, G. Chiappino, A. S. Kelus, P. G. Gell, Cellular localization of immunoglobulins with different allotypic specificities in rabbit lymphoid tissues. *J. Exp. Med.* **122**, 853–876 (1965).
7. E. Weiler, Differential activity of allelic gamma-globulin genes in antibody-producing cells. *Proc. Natl. Acad. Sci. U.S.A.* **54**, 1765–1772 (1965).
8. F. W. Alt *et al*., Ordered rearrangement of immunoglobulin heavy chain variable region segments. *EMBO J.* **3**, 1209–1219 (1984).
9. G. J. Nossal, J. Lederberg, Antibody production by single cells. *Nature* **181**, 1419–1420 (1958).
10. M. A. Eckersley-Maslin, D. L. Spector, Random monoallelic expression: Regulating gene expression one allele at a time. *Trends Genet.* **30**, 237–244 (2014).
11. A. A. Khamlichi, R. Feil, Parallels between mammalian mechanisms of monoallelic gene expression. *Trends Genet.* **34**, 954–971 (2018).
12. V. Mutzel *et al*., A symmetric toggle switch explains the onset of random X inactivation in different mammals. *Nat. Struct. Mol. Biol.* **26**, 350–360 (2019).
13. E. G. Schulz, E. Heard, Role and control of X chromosome dosage in mammalian development. *Curr. Opin. Genet. Dev.* **23**, 109–115 (2013).
14. J. T. Lee, M. S. Bartolomei, X-inactivation, imprinting, and long noncoding RNAs in health and disease. *Cell* **152**, 1308–1323 (2013).
15. J. A. Graves, Evolution of vertebrate sex chromosomes and dosage compensation. *Nat. Rev. Genet.* **17**, 33–46 (2016).
16. S. Augui, E. P. Nora, E. Heard, Regulation of X-chromosome inactivation by the X-inactivation centre. *Nat. Rev. Genet.* **12**, 429–442 (2011).
17. M. Fuxa *et al*., Pax5 induces V-to-DJ rearrangements and locus contraction of the immunoglobulin heavy-chain gene. *Genes Dev.* **18**, 411–422 (2004).
18. E. Roldán *et al*., Locus 'decontraction' and centromeric recruitment contribute to allelic exclusion of the immunoglobulin heavy-chain gene. *Nat. Immunol.* **6**, 31–41 (2005).
19. J. A. Skok *et al*., Nonequivalent nuclear location of immunoglobulin alleles in B lymphocytes. *Nat. Immunol.* **2**, 848–854 (2001).
20. C. E. Sayegh, S. Jhunjhunwala, R. Riblet, C. Murre, Visualization of looping involving the immunoglobulin heavy-chain locus in developing B cells. *Genes Dev.* **19**, 322–327 (2005).
21. S. T. Kosak *et al*., Subnuclear compartmentalization of immunoglobulin loci during lymphocyte development. *Science* **296**, 158–162 (2002).
22. B. B. Haines, P. H. Brodeur, Accessibility changes across the mouse Igh-V locus during B cell development. *Eur. J. Immunol.* **28**, 4228–4235 (1998).
23. R. J. Schlimgen, K. L. Reddy, H. Singh, M. S. Krangel, Initiation of allelic exclusion by stochastic interaction of Tcrb alleles with repressive nuclear compartments. *Nat. Immunol.* **9**, 802–809 (2008).
24. D. Kitamura, K. Rajewsky, Targeted disruption of mu chain membrane exon causes loss of heavy-chain allelic exclusion. *Nature* **356**, 154–156 (1992).
25. E. Schweighoffer, L. Vanes, A. Mathiot, T. Nakamura, V. L. Tybulewicz, Unexpected requirement for ZAP-70 in pre-B cell development and allelic exclusion. *Immunity* **18**, 523–533 (2003).

26. D. Kitamura *et al*., A critical role of lambda 5 protein in B cell development. *Cell* **69**, 823–831 (1992).
27. A. B. Eberle, K. Herrmann, H. M. Jäck, O. Mühlemann, Equal transcription rates of productively and nonproductively rearranged immunoglobulin mu heavy chain alleles in a pro-B cell line. *RNA* **15**, 1021–1028 (2009).
28. F. Papavasiliou, M. Jankovic, S. Gong, M. C. Nussenzweig, Control of immunoglobulin gene rearrangements in developing B cells. *Curr. Opin. Immunol.* **9**, 233–238 (1997).
29. F. Papavasiliou, Z. Misulovin, H. Suh, M. C. Nussenzweig, The role of Ig beta in precursor B cell transition and allelic exclusion. *Science* **268**, 408–411 (1995).
30. F. Papavasiliou, M. Jankovic, H. Suh, M. C. Nussenzweig, The cytoplasmic domains of immunoglobulin (Ig) alpha and Ig beta can independently induce the precursor B cell transition and allelic exclusion. *J. Exp. Med.* **182**, 1389–1394 (1995).
31. J. Borst, H. Jacobs, G. Brouns, Composition and function of T-cell receptor and B-cell receptor complexes on precursor lymphocytes. *Curr. Opin. Immunol.* **8**, 181–190 (1996).
32. S. Li, M. F. Wilkinson, Nonsense surveillance in lymphocytes? *Immunity* **8**, 135–141 (1998).
33. B. Baumann, M. J. Potash, G. Köhler, Consequences of frameshift mutations at the immunoglobulin heavy chain locus of the mouse. *EMBO J.* **4**, 351–359 (1985).
34. M. Bühler, A. Paillusson, O. Mühlemann, Efficient downregulation of immunoglobulin mu mRNA with premature translation-termination codons requires the 5′-half of the VDJ exon. *Nucleic Acids Res.* **32**, 3304–3315 (2004).
35. J. Lutz *et al*., Pro-B cells sense productive immunoglobulin heavy chain rearrangement irrespective of polypeptide production. *Proc. Natl. Acad. Sci. U.S.A.* **108**, 10644–10649 (2011).
36. G. Borsani *et al*., Characterization of a murine gene expressed from the inactive X chromosome. *Nature* **351**, 325–329 (1991).
37. N. Brockdorff *et al*., Conservation of position and exclusive expression of mouse Xist from the inactive X chromosome. *Nature* **351**, 329–331 (1991).
38. C. J. Brown *et al*., A gene from the region of the human X inactivation centre is expressed exclusively from the inactive X chromosome. *Nature* **349**, 38–44 (1991).
39. C. M. Clemson, J. A. McNeil, H. F. Willard, J. B. Lawrence, XIST RNA paints the inactive X chromosome at interphase: Evidence for a novel RNA involved in nuclear/chromosome structure. *J. Cell Biol.* **132**, 259–275 (1996).
40. A. Loda, E. Heard, Xist RNA in action: Past, present, and future. *PLoS Genet.* **15**, e1008333 (2019).
41. R. Galupa, E. Heard, X-chromosome inactivation: A crossroads between chromosome architecture and gene regulation. *Annu. Rev. Genet.* **52**, 535–566 (2018).
42. J. Chaumeil, P. Le Baccon, A. Wutz, E. Heard, A novel role for Xist RNA in the formation of a repressive nuclear compartment into which genes are recruited when silenced. *Genes Dev.* **20**, 2223–2237 (2006).
43. C. K. Chen *et al*., Xist recruits the X chromosome to the nuclear lamina to enable chromosome-wide silencing. *Science* **354**, 468–472 (2016).
44. C. A. McHugh *et al*., The Xist lncRNA interacts directly with SHARP to silence transcription through HDAC3. *Nature* **521**, 232–236 (2015).
45. A. Minajigi *et al*., Chromosomes. A comprehensive Xist interactome reveals cohesin repulsion and an RNA-directed chromosome conformation. *Science* **349**, (2015).
46. L. F. Zhang, K. D. Huynh, J. T. Lee, Perinucleolar targeting of the inactive X during S phase: Evidence for a role in the maintenance of silencing. *Cell* **129**, 693–706 (2007).
47. M. Simonis *et al*., Nuclear organization of active and inactive chromatin domains uncovered by chromosome conformation capture-on-chip (4C). *Nat. Genet.* **38**, 1348–1354 (2006).
48. E. Lieberman-Aiden *et al*., Comprehensive mapping of long-range interactions reveals folding principles of the human genome. *Science* **326**, 289–293 (2009).
49. L. Giorgetti *et al*., Structural organization of the inactive X chromosome in the mouse. *Nature* **535**, 575–579 (2016).
50. E. Splinter *et al*., The inactive X chromosome adopts a unique three-dimensional conformation that is dependent on Xist RNA. *Genes Dev.* **25**, 1371–1383 (2011).
51. Y. Fukita, H. Jacobs, K. Rajewsky, Somatic hypermutation in the heavy chain locus correlates with transcription. *Immunity* **9**, 105–114 (1998).
52. A. Buzina, M. J. Shulman, Infrequent translation of a nonsense codon is sufficient to decrease mRNA level. *Mol. Biol. Cell* **10**, 515–524 (1999).
53. R. Stadhouders *et al*., Pre-B cell receptor signaling induces immunoglobulin κ locus accessibility by functional redistribution of enhancer-mediated chromatin interactions. *PLoS Biol.* **12**, e1001791 (2014).
54. P. M. Dubois, J. Stepinski, J. Urbain, C. H. Sibley, Role of the transmembrane and cytoplasmic domains of surface IgM in endocytosis and signal transduction. *Eur. J. Immunol.* **22**, 851–857 (1992).
55. E. Monzón-Casanova *et al*., Polypyrimidine tract-binding proteins are essential for B cell development. *eLife* **9**, e53557 (2020).
56. Y. S. Li, K. Hayakawa, R. R. Hardy, The regulated expression of B lineage associated genes during B cell differentiation in bone marrow and fetal liver. *J. Exp. Med.* **178**, 951–960 (1993).
57. T. H. Winkler, A. Rolink, F. Melchers, H. Karasuyama, Precursor B cells of mouse bone marrow express two different complexes with the surrogate light chain on the surface. *Eur. J. Immunol.* **25**, 446–450 (1995).
58. G. S. Brouns, E. de Vries, J. Borst, Assembly and intracellular transport of the human B cell antigen receptor complex. *Int. Immunol.* **7**, 359–368 (1995).
59. L. Gauthier, B. Rossi, F. Roux, E. Termine, C. Schiff, Galectin-1 is a stromal cell ligand of the pre-B cell receptor (BCR) implicated in synapse formation between pre-B and stromal cells and in pre-BCR triggering. *Proc. Natl. Acad. Sci. U.S.A.* **99**, 13014–13019 (2002).
60. Y. Kawano *et al*., A novel mechanism for the autonomous termination of pre-B cell receptor expression via induction of lysosome-associated protein transmembrane 5. *Mol. Cell. Biol.* **32**, 4462–4471 (2012).
61. P. Krimpenfort, F. Ossendorp, J. Borst, C. Melief, A. Berns, T cell depletion in transgenic mice carrying a mutant gene for TCR-beta. *Nature* **341**, 742–746 (1989).
62. U. Grawunder *et al*., Down-regulation of RAG1 and RAG2 gene expression in preB cells after functional immunoglobulin heavy chain rearrangement. *Immunity* **3**, 601–608 (1995).
63. M. D. Robinson, D. J. McCarthy, G. K. Smyth, edgeR: A bioconductor package for differential expression analysis of digital gene expression data. *Bioinformatics* **26**, 139–140 (2010).
64. D. J. McCarthy, Y. Chen, G. K. Smyth, Differential expression analysis of multifactor RNA-Seq experiments with respect to biological variation. *Nucleic Acids Res.* **40**, 4288–4297 (2012).